arXiv:physics/0306121v3 [physics.bio-ph] 1 Oct 2005

A theory of Plasma Membrane Calcium Pump stimulation and activity

Michael Graupner[1,2]¶, Frido Erler[1] and Michael Meyer-Hermann[1,3,4]

[1]*Institute for Theoretical Physics, Dresden University of Technology, 01062 Dresden, Germany*

[2]*Laboratoire de Neurophysique et Physiologie, CNRS UMR 8119, Université René Descartes - Paris V 45, rue des Saints Pères, 75270 Paris Cedex 06, France*

[3]*Centre for Mathematical Biology, Mathematical Institute, 24-29 St. Giles, Oxford University, Oxford OX1 3LB, United Kingdom*

[4]*Frankfurt Institute for Advanced Studies (FIAS), Johann Wolfgang Goethe-University, Max von Laue-Str. 1, 60438 Frankfurt/Main, Germany*

Journal of Biological Physics 31:183-206, 2005

Abstract

The ATP-driven Plasma Membrane Calcium pump or Ca^{2+}-ATPase (PMCA) is characterized by a high affinity to calcium and a low transport rate compared to other transmembrane calcium transport proteins. It plays a crucial role for calcium extrusion from cells. Calmodulin is an intracellular calcium buffering protein which is capable in its Ca^{2+} liganded form of stimulating the PMCA by increasing both the affinity to calcium and the maximum calcium transport rate. We introduce a new model of this stimulation process and derive analytical expressions for experimental observables in order to determine the model parameters on the basis of specific experiments. We furthermore develop a model for the pumping activity. The pumping description resolves

¶To whom correspondence should be addressed, current address: Laboratoire de Neurophysique et Physiologie, Université René Descartes - Paris V, 45, rue des Saints Pères, 75270 Paris Cedex 06, France, Tel.: +33-(0)1.42.86.38.13, E-mail: michael.graupner@univ-paris5.fr

the seeming contradiction of the Ca^{2+}:ATP stoichiometry of 1:1 during a translocation step and the observation that the pump binds two calcium ions at the intracellular site. The combination of the calcium pumping and the stimulation model correctly describes PMCA function. We find that the processes of calmodulin-calcium complex attachment to the pump and of stimulation have to be separated. Other PMCA properties are discussed in the framework of the model. The presented model can serve as a tool for calcium dynamics simulations and provides the possibility to characterize different pump isoforms by different type-specific parameter sets.

Keywords: Plasma Membrane Calcium pump, Plasma Membrane Ca^{2+}-ATPase, calmodulin, stimulation, relaxation, pumping activity, theoretical model, parameter

Introduction

The Plasma Membrane Calcium pump with a high calcium affinity ($K_{1/2} < 0.5 - 1\,\mu$M [1, 2, 3]) and a low transport rate ($\approx 30\,$Hz, [4] and private communication) is an important component for the maintenance of calcium homeostasis in cells. By using the energy stored in ATP the PMCA transports intracellular calcium ions out of the cell. It has been found in all mammalian cells [5], where the expression level does not exceed 0.1% of the total membrane protein [1, 6, 7, 8]. An exception is the brain where this value is up to 10 times higher than in non-excitable cells [5].

The four different pump isoforms are encoded by four independent genes, which are indicated by numbers 1-4. The diversity of pump forms is further increased by alternative mRNA splicing variants, characterized by small letters. There exist more than 26 transcripts which differ in their regulatory properties, for instance in their affinity to calmodulin, and which are distributed in a tissue specific manner [1, 3]. Referring to the available data we will investigate hPMCA2b and hPMCA4b, where h stands for human [9].

Calmodulin is an intracellular calcium sensor protein with four relatively high affinity Ca^{2+} binding sites ($K_a = 1 - 10\ \mu\text{M}^{-1}$ at low ionic strength [10]). It belongs to the mobile proteins of the EF-hand family with a helix-loop-helix conformation [11]. Two calcium ions are bound at the N-terminal as well as at the highly homologous C-terminal domain, each of them formed by two EF-hands [8]. The domains are connected by a flexible linker - an α-helix [8]. Because of its calcium binding capacity calmodulin becomes relevant for the spatial propagation of calcium signals within the cytoplasm. Additionally the fully liganded

calmodulin-calcium complex is responsible for Ca^{2+}-dependent regulation of the activities of a vast array of different target proteins, including enzymes, ion pumps and channels [12]. Among those with high affinity (K_d = 5 nM) to the calmodulin-calcium complex is the PMCA [13]. The free calmodulin-binding domain of the PMCA also interacts with the ATP-binding site of the pump and acts as an inhibitor of ATP-driven pump function [7, 14]. The detachment of that autoinhibitory domain segment after binding of the complex causes a stimulation of the pump function by increasing both the affinity to calcium and the maximum turnover rate of calcium [2, 3, 8, 15]. The stimulation and the relaxation to the initial unstimulated state happens on a time scale of minutes and enables the pump to display a memory of previous calcium transients [9].

Caride *et al.* have published a stimulation model making use of measurements of the dynamical stimulation behavior [9]. We extend the reaction scheme and aim to improve the model results in two ways: Firstly, we will deduce the stimulation parameters from measured data. Secondly, we will include a saturation of the stimulation rate for high calcium concentrations. Indeed, measured stimulation constants call for a limitation by a maximum value at high calcium concentrations. After completion of this work we were made aware of the recently published article in which Penheiter *et al.* propose a new stimulation model in conjunction with fluorescence measurements [16]. Although Penheiter's model includes saturation, the relaxation of the PMCA to resting state is not considered. We separate the stimulation as well as the relaxation into two steps and introduce rate limiting reactions in our model. An analytical approach enables us to deduce the required rate constants from measurements. The inferred system of coupled nonlinear differential equations is solved numerically. The presented new model is in agreement with the investigated experimental data of the stimulation process by calmodulin. Furthermore we predict the stimulation behavior beyond the available data.

Besides the stimulation model we also consider the calcium pumping activity. This joined model of stimulation and pumping may serve as a tool for simulations in a wide variety of systems such as single cells or tissues. For that purpose we assume that all isoforms are functionally similar and characterize the different isoforms by type specific sets of parameters. In this way we differentiate between universal system independent parameters which are characteristic for each pump type and specific parameters such as the PMCA protein expression level, which has to be adapted to each experimental setup.

In relation to the available experiments we can specify parameter sets for the h2b and h4b isoform which turn out to be in a biologically reasonable range.

We begin by introducing the stimulation model reactions. We determine the model parameters and calculate stimulation dynamics. In the second part of this paper we focus on the derivation of an expression for the calcium pumping activity. Finally the stimulation and the pumping model together serve to fully describe PMCA function.

Model

Stimulation model

We base the stimulation model on a system of rate reactions, which describe the calcium and calmodulin dependent transition from unstimulated to stimulated pump form and vice versa. The stimulation dynamics of an ensemble of PMCA's is characterized by the following reactions:

$$\mathrm{M} + 4\mathrm{Ca}^{2+} \underset{k_{-1}}{\overset{k_1}{\rightleftharpoons}} \mathrm{X}_4, \tag{1}$$

$$\mathrm{P} + \mathrm{X}_4 \underset{k_{-2}}{\overset{k_2}{\rightleftharpoons}} \mathrm{P}_\mathrm{X}, \tag{2}$$

$$\mathrm{P}_\mathrm{X} \overset{k_3}{\rightharpoonup} \mathrm{P}^*_\mathrm{X}, \tag{3}$$

$$\mathrm{P}^*_\mathrm{X} \underset{k_{-4}}{\overset{k_4}{\rightleftharpoons}} \mathrm{P}^* + \mathrm{X}_4, \tag{4}$$

$$\mathrm{P}^* \overset{k_5}{\rightharpoonup} \mathrm{P}. \tag{5}$$

We use the following abbreviations: P denotes free PMCA, $\mathrm{CaM{\cdot}Ca_4} \equiv \mathrm{X_4}$, $\mathrm{P{\cdot}CaM{\cdot}Ca_4} \equiv \mathrm{P_X}$, $\mathrm{P^*{\cdot}CaM{\cdot}Ca_4} \equiv \mathrm{P^*_X}$, and P^* free stimulated pump. P and $\mathrm{P_X}$ are the unstimulated pumps and the asterisk denotes stimulated pumps. M and Ca^{2+} are free intracellular calmodulin and calcium, respectively. Note that in this article Roman style symbols refer to elements or proteins whereas italic style symbols denote concentrations or fractions of the respective element or protein. The k's are the rate constants. With the Law of Mass Action the model (1)-(5) is rewritten as a set of differential equations for concentrations (see equations (16)-(18) in the Appendix for the stimulation model).

Reaction (1) describes the binding of calcium to calmodulin. The cooperative binding of Ca^{2+} within each domain of the calmodulin protein [10] is simplified in this reaction by the assumption of highly cooperative binding of all four calcium ions. Based on the realistic assumption that the binding of calcium occurs faster than the PMCA stimulation, which happens on a time scale of minutes, we treat this binding to be in quasi-steady-state.

The assumption of irreversible stimulation (3) and relaxation (5) implies that the pump can only be stimulated when X_4 has attached to the pump, whereas recovery back to the unstimulated pump form only occurs when X_4 has detached. It will be seen later on that the irreversible step (3) and the detachment step (4) limit the stimulation and relaxation rate, *i.e.* both cannot exceed the rates k_3 and k_4, respectively. Note that (4) does not necessarily mean that the complex detaches as a whole. In principle the calcium ions could also detach from P_X^* first without any alterations of the model because of the quasi-steady-state approximation in (1). Thus, the essential statement of (4) is that calmodulin (with or without calcium) has to detach in order to destimulate the pump.

Note that we introduced different pathways for the stimulation (reactions (2) and (3)) and the relaxation process (reactions (4) and (5)). This enables us to describe the temporal behavior of these two processes independently of each other, which is rather important in order to reflect isoform specific stimulation and relaxation dynamics.

Stimulation model parameter determination We aim to relate the rate constants $k_i \quad (i = \pm 1, \pm 2, 3, \pm 4, 5)$ and the stimulation and relaxation constants $k_{\text{stim}}^{\text{exp}}$ and $k_{\text{relax}}^{\text{exp}}$ measured in experiment by Caride *et al.* [9]. Note that in [9] these constants are denoted by k_{act} and k_{inact}, respectively. Starting from the stimulation model we deduce analytical expressions for the exponential growth constants k_{stim} and k_{relax}.

Stimulation Suppose only unstimulated pump form P to be present with the subsequent addition of calmodulin. In the very beginning the stimulation model can be reduced to the rate equations (1), (2) and (3). The binding of calcium to calmodulin (reaction (1)) is assumed to be in quasi-steady-state, therefore $X_4 \equiv CaM{\cdot}Ca_4 = K \cdot M \cdot Ca^4$, with $K = k_1/k_{-1}$. During the beginning of the stimulation the finite calmodulin concentration imposes no restrictions on the dynamics, since only a minor fraction of free X_4 is bound. Therefore, the conservation of the calmodulin concentration is neglected and M is considered to be constant. With this assumption and the pump mass conservation $P_0 = P + P_X + P_X^*$ (note that P^* is not involved here) reactions (2) and (3) can be rewritten as a system of three linear homogeneous differential equations of first order (the full nonlinear system is shown in equations (16)-(18) in the Appendix). The system is solved via the ansatz $P = A_1 \cdot exp(-k_{\text{stim}}t)$, $P_X = A_2 \cdot exp(-k_{\text{stim}}t)$ and $P_X^* = A_3 \cdot exp(-k_{\text{stim}}t)$.

The characteristic equation leads to three solutions for k_{stim}: $k^1_{\text{stim}} = 0$ and

$$k^{(2/3)}_{\text{stim}} = \frac{k_{-2} + k_3 + k_2 X_4}{2} \pm \sqrt{\left(\frac{k_{-2} + k_3 + k_2 X_4}{2}\right)^2 - k_2 k_3 X_4}. \tag{6}$$

With the boundary conditions $P(0) = P_0$, $P(\infty) = 0$, $P_X(0) = 0$, $P_X(\infty) = 0$, $P^*_X(0) = 0$, $P^*_X(\infty) = P_0$ and the pump mass conservation $P_0 = P(t) + P_X(t) + P^*_X(t)\ \forall\ t$, the exact solution for the stimulated pump form becomes

$$P^*_X(t) = P_0 \left[1 + \left(\frac{k^{(2)}_{\text{stim}}}{k^{(3)}_{\text{stim}}} - 1\right)^{-1} e^{-k^{(2)}_{\text{stim}} t} - \left(1 - \frac{k^{(3)}_{\text{stim}}}{k^{(2)}_{\text{stim}}}\right)^{-1} e^{-k^{(3)}_{\text{stim}} t}\right]. \tag{7}$$

During the first phase of stimulation the pump exhibits a single exponential behavior as discussed in [17]. The exact solution for $P^*_X(t)$ in equation (7) can be simplified to a single exponential expression in two cases. With $k^{(2)}_{\text{stim}} >> k^{(3)}_{\text{stim}}$ equation (7) becomes

$$P^*_X(t) = P_0(1 - e^{-k^{(3)}_{\text{stim}} t}). \tag{8}$$

Formally, also $k^{(2)}_{\text{stim}} << k^{(3)}_{\text{stim}}$ yields a single exponential behavior of the same form but with $k^{(2)}_{\text{stim}}$ in the exponent. However, $k^{(2)}_{\text{stim}} \geq k^{(3)}_{\text{stim}}$ holds true (see equation (6)).

Assuming $k^{(2)}_{\text{stim}} >> k^{(3)}_{\text{stim}}$ the formation of the stimulated pump form during the first phase of stimulation depends on $k^{(3)}_{\text{stim}}$ only. This approximation is supported by the fact that $k^{(3)}_{\text{stim}}$ converges at high calcium concentrations in the same manner as $k^{\text{exp}}_{\text{stim}}$ does (see figure 1). In contrast, $k^{(2)}_{\text{stim}}$ diverges for high calcium concentrations (see Appendix). $k^{(3)}_{\text{stim}}$ figure 1
can be interpreted as corresponding to the single exponential fit constant $k^{\text{exp}}_{\text{stim}}$. This enables us to determine the stimulation parameters (shown in figure 1).

In an analogous fashion to the stimulation case we deduce an analytical expression like equation (8) for the relaxation scenario. The exponent of this single exponential expression can be related to the experimentally measured relaxation constant (see figure 2, calculation not shown). figure 2

A fit of the derived expressions for the introduced stimulation parameters to the experimental data restricts their values. As a first approach we use Hill equations (see Appendix for the stimulation case). The maximum stimulation and relaxation fit constant can be identified with k_3 and k_4, respectively, which limits the stimulation and relaxation rate. In contrast, the half maximum concentration of the Hill fit is not sufficient to determine the remaining free parameters. Even with the knowledge of the dissociation constant K_2, $K_2 = k_{-2}/k_2 = 0.5$ nM for the h2b isoform and $K_2 = 5$ nM for the h4b isoform

[5, 9, 13, 15, 18, 19, 20], the system remains under-determined because K is not precisely known. A lower boundary for K comes from the requirement of positive reaction rates k_2 and k_{-2} and from the value of K_2. An upper boundary for K is imposed by the choice of the value for $K_4 = k_4/k_{-4}$. The parameters resulting from the Hill equation fits are reported in table 1. table 1

Attention should be drawn to the fact that Ca^{2+} is bound by polar amino acids of calmodulin and therefore the affinity represented by K strongly depends on the ionic strength of the experimental solution [10]. We assume the same value of K for all experiments, i.e. the same conditions in all experiments. Since the value of K is not exactly known for the experiments under consideration, we assume three different values and quote the respective parameter sets in order to show how other parameters depend on K. The values used for K are 0.1, 1 and 10 μM^{-4} which, according to Linse *et al.*, correspond to an experimental solution with a KCl concentration of 18, 20 and 26 mM.

Using (6) and the parameter values determined by the Hill equation fit we are able to calculate the calmodulin dependence of k_{stim} without further assumptions. The result in figure 1 (dotted line) is in qualitative agreement with the experimental data of figure 3B in [16] (k_{act}). The measurements have been carried out at a calcium concentration of 10 μM with 0.005-0.065 μM calmodulin. The experimental data could be fitted by a linear equation. The saturation suggested in figure 1 occurs at higher calmodulin concentrations only. A linear fit is also suggested in figure 4A in [21] for a range of 0.005-1.25 μM calmodulin at a constant calcium concentration of 1 μM. However, the linearity of the fit relies on a single data point and we consider this result to be in agreement with the saturation predicted by our model. We quote k_{stim} at a calcium concentration of 0.8 μM for the h2b isoform and at 1 μM for h4b. At both cases the stimulation constant saturates already at low calcium concentrations, *i.e.* at ≈ 0.2 μM for h2b and at ≈ 0.4 μM for h4b. The results from the Hill equation fit also allow us to predict the calmodulin dependence of the relaxation constant k_{relax}, which has not been measured so far (see figure 2).

We have seen that it is not possible to reliably determine all stimulation parameters by a fit on the basis of Hill equations. We therefore use a Metropolis algorithm, which is based on a least-squares fit routine, to incorporate three sets of available data for the stimulation constant, the relaxation constant and, in addition, the steady-state pumping activity, which will be discussed subsequently. The medians and the confidence intervals in table 2 and 4

are calculated from a Bootstrap method, *i.e.* random data sets of the same size are drawn from the original data set from which, using the Metropolis algorithm, the fit parameters are calculated. Repeating this procedure 10.000 times enables us to calculate medians and confidence intervals for the fit parameters. The medians of the parameters in table 3 are determined similarly but for different values of K. table 2 table 3

Note that we have derived equation (6) only by considering the beginning of the stimulation. An alternative approach to determine the parameters would be the fit of the exact model equations to the time course of inorganic phosphate Ph_i release (whereas sub-i refers to inorganic). Ph_i emerges by hydrolyzing ATP during pumping (see section "Results" and [9, 17]). However, this would not improve the accuracy of the parameter determination since these data contain information not only about the stimulation but also about the pumping of the PMCA, which cannot be disentangled. Only a measurement of the exact stimulation and relaxation behavior would provide relevant additional information in order to get a more reliable choice in table 2.

Stimulation dynamics Based on the stimulation model reactions (1)-(5) we can simulate the dynamics of the unstimulated and stimulated PMCA states. With the obtained isoform specific parameters differences between the isoforms can be discussed. The fact that the value of k_3 for the h2b isoform is more than twice that of the h4b isoform reflects faster stimulation, whereas relaxation is faster for the h4b isoform since $k_4^{h4b} > k_4^{h2b}$. The stimulation and relaxation dynamics of both isoforms are shown in figure 3. In graph 3 (a) we start with no stimulated pump (i.e. $f_{\mathrm{stim}}(t_0 = 0) = 0$) and expose the pump to a high calcium concentration. In the relaxation graph 3 (b) all pumps are stimulated (i.e. $f_{\mathrm{stim}}(t_0 = 0) = 1$) and the calcium concentration is decreased to 0.1 μM. figure 3

Pumping model

Up to this point we have described the temporal transition between unstimulated and stimulated pump forms. In this section we will mathematically characterize how the PMCA transports calcium ions across the membrane depending on the intracellular calcium concentration. We will consider the pump cycle to be in quasi-steady-state, *i.e.* the pump activity reacts immediately to the intracellular calcium concentration. This simplification is justified since the pump activity adapts to different calcium concentrations within milliseconds

while the stimulation and relaxation happens on a time scale of minutes.

Pumping activity In contrast to the Ca^{2+} pump of the sarcoplasmic reticulum (SERCA) the stoichiometry between transported Ca^{2+} and hydrolyzed ATP of the PMCA is most likely 1:1 [1, 3, 7, 22]. The SERCA pump works with a calcium:ATP ratio of 2:1 [7, 22]. Hence, the transport step of one calcium ion through the plasma membrane becomes

$$\mathrm{P_{in}} \xrightarrow{\mathrm{r_1}} \mathrm{P_{out}} + \mathrm{Ca^{2+}_{out}}. \tag{9}$$

$\mathrm{P_{in}}$ stands for a state of the pump in which one or two calcium ions are bound and which can perform the calcium transport process by a transformational change. $\mathrm{P_{out}}$ refers to the pump state after the translocation step. We do not consider the transformational change from $\mathrm{P_{out}}$ to $\mathrm{P_{in}}$, which closes the pump cycle. Since ATP is assumed to be sufficiently available in cells we treat the ATP concentration as thermodynamical bath. The calcium transport rate J in the outward direction is given by

$$J = r_1 \cdot P_{\mathrm{in}}. \tag{10}$$

Carafoli pointed out that the activation of the ATPase by calcium and the saturation can best be described by a Hill equation with a Hill coefficient of two [3]. This may be related to the binding of 2 calcium ions at the intracellular binding site of the pump even if only one calcium ion is translocated. In the following this is incorporated into the model:

$$\mathrm{P} + \mathrm{Ca^{2+}} \underset{\mathrm{r_{-2}}}{\overset{\mathrm{r_2}}{\rightleftharpoons}} \mathrm{P{\cdot}Ca}, \tag{11}$$

$$\mathrm{P{\cdot}Ca} + \mathrm{Ca^{2+}} \underset{\mathrm{r_{-3}}}{\overset{\mathrm{r_3}}{\rightleftharpoons}} \mathrm{P{\cdot}Ca_2}. \tag{12}$$

The pump state $\mathrm{P_{in}}$ is assumed to comprise the pumps with one and two calcium ions, *i.e.* $\mathrm{P_{in}} = \mathrm{P{\cdot}Ca} + \mathrm{P{\cdot}Ca_2}$. This implies that the pump with one calcium ion, $\mathrm{P{\cdot}Ca}$, is able to perform the transport process which is not necessarily the case but the most general assumption (see also comments after equation (14)).

In the quasi-steady-state approximation of equations (11) and (12) we find an expression for P_{in}. Using this expression the calcium transport rate (equation (10)) becomes

$$J = r_1 \frac{R_3 Ca + Ca^2}{R_2 R_3 + R_3 Ca + Ca^2}, \tag{13}$$

with $R_2 = r_{-2}/r_2$ and $R_3 = r_{-3}/r_3$ and the pump mass conservation $1 = P + P{\cdot}Ca + P{\cdot}Ca_2$. Note that we have divided the pump mass conservation by $\mathrm{P_0}$ so that the different pump

states become fractions instead of concentrations. The sum of the fractions of all the three pump states is of course 1.

Fitting equation (13) to the experimentally measured transport rate in the absence of calmodulin yields $R_2 = 38\ \mu$M and $R_3 = 0.011\ \mu$M for the h2b isoform (see figure 4). These values suggest a cooperative binding of both calcium ions, *i.e.* the binding of the first ion is slow but of the second fast. In the model this means $r_2 \to 0$ and $r_3 \to \infty$ while keeping $r_2 \cdot r_3$ constant, in which case $R_2 \to \infty$ and $R_3 \to 0$ while $R_2 R_3$ is constant. Experiments performed by Elwess *et al.* [15] or by Verma *et al.* [23] yield the same sigmoidal behavior of the transport rate as found by equation (13) in figure 4, supporting the assumption of cooperative binding. Thus (13) is simplified to

$$J = r_1 \frac{Ca^2}{R_2 R_3 + Ca^2} = J_{\max} \frac{Ca^2}{{H_{1/2}}^2 + Ca^2}. \tag{14}$$

In this expression the pumping activity of the P·Ca state which has only one calcium ion bound is neglected. The high cooperativity prevents us from deciding whether this state is contributing to the total pump activity or not.

Equation (14) has the form of a Hill equation with Hill coefficient $n = 2$. r_1 can be identified with the maximal pump rate $J_{\max}$. Since the maximum rate of the calcium pumping is limited by r_1 in equation (14), $r_1 = J_{\max}$ stands for the saturating properties of the pumping process. $H_{1/2} = \sqrt{R_2 R_3}$ is the half activation concentration and a measure for the affinity of the pump to calcium. We will use equation (14) for all further investigations in this paper.

So far we have only looked at the calcium-dependent pump activity in the absence of calmodulin without considering pump stimulation. The activity in the unstimulated state corresponds to the base activity in the absence of calmodulin. It is very likely that the interaction with calmodulin causes the increase in pumping activity since it is well-known that calmodulin increases both the affinity for calcium as well as the maximal activity and both effects occur during stimulation [16]. The transition dynamics is given by the stimulation model in equations (1)-(5). Hence, the total pumping rate of a system becomes

$$J = f_{\text{unstim}} \cdot \frac{J_{\max} \cdot Ca^2}{{H_{1/2}}^2 + Ca^2} + f_{\text{stim}} \cdot \frac{J^*_{\max} \cdot Ca^2}{{H^*_{1/2}}^2 + Ca^2}, \tag{15}$$

where f_{unstim} and f_{stim} are the fractions of unstimulated and stimulated pump with $f_{\text{unstim}} = \frac{P+P_X}{P_0}$ and $f_{\text{stim}} = \frac{P^*+P^*_X}{P_0}$.

One input parameter of the stimulation model is the total pump concentration P_0. This concentration P_0 is taken from Caride *et al.* [9] to be $0.005\,\mu$M. Assuming a sufficiently large amount of pumps, the total pump concentration is irrelevant for the pumping model since we consider fractions of pumps in different states only. In contrast in the stimulation model the proportion between the total calmodulin concentration, M_0, and the total pump concentration, P_0, is significant. If for example the amount of PMCA's exceeds the number of available calmodulin proteins not all pumps could be stimulated.

For simulations the surface density of PMCA's has to be transfered into the concentration P_0. This implies the neglection of diffusion of the calcium-calmodulin complex to and from the pump, which is justified for rather small compartments only. For larger compartments a space resolving model with a local pump concentration has to be used.

Pumping parameter determination with steady-state pump activity By setting all differential equations (equations (16), (17) and (18), see Appendix) of the stimulation model (reactions (1)-(5)) to zero the steady-state distribution of P, $\mathrm{P_X}$, $\mathrm{P_X^*}$ and $\mathrm{P^*}$ is found. This determines the asymptotic steady-state fractions f_{unstim} and f_{stim} in equation (15). Using this distribution we calculate the asymptotic pumping activity in dependence of the calcium and calmodulin concentration. Many measurements of the steady-state pump activity in the presence and the absence of calmodulin have been performed [9, 19, 23, 24, 25]. Fitting equation (15) to one of these experiments yields $J_{\max}$, $J^*_{\max}$, $H_{1/2}$ and $H^*_{1/2}$. In figure 4 we use the steady-state activity measurements done by Caride *et al.* [9]. figure 4

With $f_{\mathrm{unstim}} = 1$ and $f_{\mathrm{stim}} = 0$ in equation (15) we fit the steady-state activity curve in the absence of calmodulin which supplies $J_{\max}$ and $H_{1/2}$ in equation (14). Equation (15) is used to fit the data in the presence of calmodulin (see dashed line in figure 4). We determine $J^*_{\max}$ and $H^*_{1/2}$ with that fit, whereby the steady-state fractions f_{unstim} and f_{stim} are determined by the stimulation model. These fractions respect the fact that at lower calcium concentrations in the presence of calmodulin no stimulated pump form is available ($f_{\mathrm{stim}} \simeq 0$). This can be seen by inspecting the dashed-dotted line in figure 4, which is plotted with the artificial assumption that only stimulated pump form ($f_{\mathrm{stim}} = 1$) is present for all calcium concentrations. The gap between this virtual line (dashed-dotted) and the fit of equation (15) (dashed line) at low calcium concentrations is determined by the choice of the stimulation parameter set of table 2. Although we determine $J^*_{\max}$ and $H^*_{1/2}$ with

that fit, changes in $J^*_{\max}$ and $H^*_{1/2}$ only alter the slope and the saturation value whereas the gap at low calcium concentrations is not influenced by these changes: $J^*_{\max}$ and $H^*_{1/2}$ do not alter the low calcium concentration limit. Note that the fit of the case with calmodulin being present, and therefore the determination of $J^*_{\max}$ and $H^*_{1/2}$, is accomplished with the Bootstrap method using the Metropolis fit algorithm that also takes into account the stimulation and relaxation constant data sets. The pumping parameters obtained from this routine are summarized in table 4. The impact of stimulation by calmodulin on PMCA function, namely to increase both the affinity to calcium $H_{1/2}$ and the maximum pump rate $J_{\max}$, can be affirmed. table 4

The obtained parameters $J_{\max}$ and $J^*_{\max}$ refer to the investigated system, *i.e.* they are determined by the ensemble of investigated pumps. In contrast to the pump rate, the affinity to calcium expressed by $H_{1/2}$ or $H^*_{1/2}$ is a universal parameter since it does not depend on the surface density. Knowing the expression level of PMCA's within the system and the average protein mass one can use $J_{\max}$ and $J^*_{\max}$ to calculate the maximum unstimulated J_{single} and stimulated pumping rate J^*_{single} of a single pump respectively, which is then a system-independent parameter characteristic for the isoform studied. Caride *et al.* achieved with the baculovirus expression system an amount of 5% PMCA's of total membrane protein (private communication). With this data and with an overall average protein mass of 130 kDa [7] we deduced a turnover rate of 10.4 Hz out of $J^*_{\max} = 0.24\,\mu\text{mol}/(\text{mg}\cdot\text{min})$ for the h2b isoform and 31.7 Hz out of $J^*_{\max} = 0.73\,\mu\text{mol}/(\text{mg}\cdot\text{min})$ for the stimulated h4b rate.

With the use of the pumping parameters and the stimulation rate constants (table 2) we can calculate the calmodulin dependence of the steady-state activity (see figure 5). The displayed fractional steady-state activity f is a universal description, *i.e.* it is not figure 5 dependent on the surface density. The quantitative behavior of our calculation is confirmed by experimental data of Penheiter *et al.* [20] (compare our figure 5 with figure 3 on page 17730 in this publication). Note that we calculated this steady-state activity out of the available data without further fitting routines.

Results

Comprehensive PMCA dynamics With the knowledge of the stimulation parameters from table 2 and the pumping properties in table 4 we are now able to simulate the time

dependent behavior of the calcium pumping rate of the PMCA including the stimulation.

In a corresponding experiment [9] tissue with PMCA pumps of isoform h2b was exposed consecutively to different calcium concentrations. The time course of Ph_i produced is shown in figure 6 (a) (crosses). It is rather likely that during a single turnover of the PMCA one ATP is hydrolyzed as well as one calcium ion transported [1, 2, 3, 7]. Therefore the rate of Ph_i production directly corresponds to the calcium pumping rate. Utilizing equation (15), we can calculate and sum up the time course of Ph_i production. With the use of the universal parameter sets we adapt our simulation (full line in figure 6) to this experiment by adjusting the unknown surface density of PMCA's. This yields an expression level of 9.8 % PMCA's of total membrane protein, which is comparable to the quoted 5 % (see before). Note that we have added a constant base level rate with respect to the non-zero Ph_i production rate in the absence of calcium ($Ca = 0\,\mu\mathrm{M}$) in figure 6 (a), which has to be related to a different source within the investigated tissue. In fact, in the absence of calcium no ions can be transported, *i.e.* no ATP can be hydrolyzed, no Ph_i produced. Note that during the second exposure to 0.5 μM calcium the measured activity significantly decreases compared to the first time at high calcium concentration, *i.e.* even under the same experimental conditions the Ph_i production rate changes during the experiment. This might be related to dwindling resources such as ATP or the increasing significance of ATP and calcium diffusion. Such effects naturally cannot be reproduced by the present model.

figure 6

After 300 seconds at 0.5 μM calcium, during which a PMCA fraction is stimulated, the concentration was decreased to 0.05 μM calcium for different durations and raised again to high calcium concentration. The turnover rate at the end of the second low calcium exposure $J_{0.05}^{(\mathrm{second})}$ is, due to the gradual decay of stimulated pump form, dependent on the duration of the low calcium phase. The fraction of change in $J_{0.05}$, $\frac{J_{0.05}^{(\mathrm{second})} - J_{0.05}^{(\mathrm{first})}}{J_{0.5}^{(\mathrm{first})} - J_{0.05}^{(\mathrm{first})}}$ is shown in figure 6 (b). The temporal behavior of pump function is quantitatively reproduced.

Discussion

Our combined model of stimulation and pumping is able to reproduce the PMCA behavior. Therefore the assumptions of the stimulation model could serve as a possible explanation for the underlying biological steps. An essential element of the model is the separation of the attachment of the calmodulin-calcium complex to the pump (reaction (2)) and the stimula-

tion, which occurs in an additional step (reaction (3)). The convergence of the stimulation constant $k_{\mathrm{stim}}^{\mathrm{exp}}$ at high calcium concentrations in figure 1 provides strong evidence for that assumption. The translocation step in reaction (9) has the same characteristics. These steps can be seen as internal conformational changes where their velocity cannot be further increased by higher concentrations. In contrast to reaction (3) which is confined by the total available pump concentration P_0 and k_3, the velocity of reaction (2) can be arbitrarily increased with higher calcium or calmodulin concentrations. Similarly the saturation of the relaxation constant $k_{\mathrm{unstim}}^{\mathrm{exp}}$ at low calcium concentrations calls for a rate limiting reaction during relaxation. Regarding the relaxation pathway in this context yields two steps which could meet this property, *i.e.* forward reaction (4) and reaction (5). The Metropolis fit algorithm provides similar outcomes for both possibilities. In general the routine delivers $k_4 < k_5$, *i.e.* reaction (4) limits the relaxation rate. The experimental data could also be reproduced assuming $k_4 > k_5$, which corresponds to the irreversible relaxation being the limiting step. However, figure 4b in [16] provides clear evidence that the limiting step is related to the dissociation of calmodulin, hence step (4) in our model.

The separation between stimulation (reactions (2) and (3)) and relaxation (reactions (4) and (5)) enables us to describe the different temporal behaviors independently. This is required since for example the isoforms h2b and h4b display opposite stimulation and relaxation behavior: The h2b isoform is stimulated more quickly than h4b but relaxes more slowly under the same conditions. Assuming the stimulation reaction (3) would become reversible, the formation and degradation of stimulated pump form $\mathrm{P_X^*(t)}$ could be described together by the first three reactions (1), (2) and (3) without the use of reactions (4) and (5). In such a case the calcium and calmodulin dependent stimulation and relaxation velocity could not be adjusted autonomously which is required for the reproduction of the experimental data. The formal introduction of two different pathways may be interpreted as different underlying transformational changes.

Comparing our parameters with those of the model proposed by Penheiter *et al.* in [16] reveals strong agreement. These authors argue that the preferred stimulation route in their branched model is the binding of the $\mathrm{X_4}$ complex to the unstimulated (closed, in their terminology) conformation and the subsequent stimulation (opening) of the pump. This corresponds to our single stimulation step. The second route assumes a stimulated (open) state of the pump in the absence of the $\mathrm{X_4}$ complex which would be stabilized by the binding

of the calmodulin-calcium complex. This branch had to be introduced in [16] in order to describe the initial increase in fluorescence. As in our model, the conformational change limits the stimulation. The limiting steps of the Penheiter *et al.* model are determined by k_1^{p} and k_4^{p}, where k_4^{p} describes the preferred stimulation route (here p refers to reaction rates in the Penheiter model). The value for $k_4^{\mathrm{p}} = 0.034$ 1/s is similar to our k_3 (see h4b isoform in table 1 and 2). Their and our model confirm the known affinity of the h4b isoform for the calmodulin-calcium complex [13, 17, 18, 20].

Since we have based the parameter deduction on inorganic phosphate, Ph_i, release measurements and the Penheiter model relies on fluorescence measurements based on the binding of calmodulin to the pump, the agreement of the parameters justifies both approaches. However, the reduction of the Penheiter model to the stimulation pathway ending in a stimulated pump with isomerized CaM protein (TA-CaM-PMCA$_0^*$) might not account for the competing stimulation and relaxation processes of the pump. This fact together with the branched model ansatz could be the reason for slightly different reaction rates.

As already mentioned, the choice of k_i (i= $\pm 2, 3, \pm 4, 5$) and therefore the choice of K has a sensitive effect on the stimulation and relaxation graphs in figure 1 and 2. Furthermore the steady-state graphs in figure 4 are strongly influenced by these parameters. The attempt to reproduce all experimental data for both isoforms on the basis of our model by using a single value of K leads us to the following conclusion: The affinity of the PMCA for the X_4 complex is altered during the stimulation process. The unstimulated pump P exhibits a lower affinity than the stimulated pump P* (compare $K_2 = k_{-2}/k_2$ to $K_4 = k_4/k_{-4}$). For both isoforms the value of K_4 is thousandfold lower compared to K_2 ($K_4 = 0.0008$ nM for h2b, $K_4 = 0.002$ nM for h4b). Within the framework of our model the assumption $K_2 = K_4$ fails to adequately reproduce all experimental data. In the case of the isoform h4b this assumption does not allow a sufficient amount of PMCA to become stimulated in the steady-state calculation. In principle the experimental data in figure 4 could still be fitted by adjusting $H_{1/2}^*$ and $J_{\max}^*$, but this would contradict the statement that $J_{\max}$ is about 20% of $J_{\max}^*$ for the h4b isoform [9, 15, 19, 20]. Note that this result is indirectly supported by the observation that the Ca^{2+}/calmodulin-dependent protein kinase II (CaMKII) target protein has a thousandfold higher affinity to the X_4 complex in the stimulated state, an effect denoted as calmodulin trapping [26].

The fit results in table 3 show that apart from k_2 and k_5 the parameters remain relatively

constant for different values of K. Hence, an exact determination of K under the specific experimental conditions could improve the determination of k_2 and k_5 but would not change the remaining values of the stimulation, the pumping parameters or the main conclusions. Note, that for all of the three assumed values, *i.e.* $K = 0.1$, 1 and 10 $1/\mu\mathrm{M}^4$, the experimental data of both isoforms could be reproduced with equal accuracy.

We have also investigated a different approach for PMCA relaxation. In this scenario only calcium dissociates from the complex P_X^* in step (4)'. The following reaction (5)' comprises the relaxation and the detachment of calmodulin. Though the reproduction of the available experimental data is ensured with this approach, there are two aspects which distinguish it from the present model. First, the analytical expression for the relaxation constant becomes independent of calmodulin due to the irreversibility of step (5)'. It is, therefore, impossible to predict the calmodulin dependence of the relaxation rate as done in figure 2. Second, similar to the change of the pump affinity for the X_4 complex in the present model, the affinity of calmodulin for calcium would be different depending on whether calmodulin is free (reaction (1)) or bound to the PMCA pump (reaction (4)'). We can find experimental support for both scenarios. As previously quoted, CaMKII is known to change its affinity for the calmodulin-calcium complex [26], whereas Olwin *et al.* report a change of the dissociation constant between CaM and calcium over two orders of magnitude in the presence and in the absence of a target protein, *i.e.* in their case the rabbit skeletal muscle myosin light chain kinase [27]. No experimental evidence is known to us whether calcium or the whole X_4 complex detaches first from the pump. However, since we treat the balance between free X_4, calmodulin and calcium in quasi-steady-state our approach presented here is the more general one since reaction (4) makes only the statement that the detachment of calmodulin limits the relaxation rate but does not restrict in which order the components dissociate.

In the description of the pumping behavior we have incorporated the experimental observations that although the translocation step involves only one calcium ion (indicated by the 1:1 stoichiometry of ATP to transported calcium) the pump binds two Ca^{2+} ions with high affinity [1, 2, 3, 7]. The experimental data provide strong evidence for the assumption that the binding of the two calcium ions to the intracellular binding site of the pump is highly cooperative. The deduced pumping rate expression is in accordance with these observations. The high cooperativity prevents us from determining whether only $\mathrm{P{\cdot}Ca_2}$

or also P·Ca can perform the transport process of one calcium ion. Our general ansatz could in principle account for recent findings of Guerini *et al.* in which the Ca^{2+}-dependent ATPase activity is fitted by a Hill function with Hill coefficient 1 [28]. However, the fit to the available data (see figure 4) suggests a Hill coefficient 2.

Our aim to characterize pump isoforms by different universal parameter sets is achieved for the h2b and h4b isoforms. We assume the same functionality for all isoforms, hence these parameters express relevant differences in the stimulation and pumping behavior. With the concept of providing universal parameter sets we claim that the sets are applicable to other simulations including hPMCA2b or hPMCA4b isoforms.

Out of the universal parameters of the h4b isoform we can calculate an accurate prediction of the calmodulin dependence of the steady-state activity. Using the expression level and the overall average protein mass we calculated single pump turnover rates. Based on a measurement of Elwess *et al.* in 1997 [15] and using an expression level of 0.2 % we computed a turnover rate of 8.5 Hz for the rPMCA2b isoform. Our calculated single turnover rates (table 4) are in the same range as those of Blaustein who indicated a turnover of $\approx$ 30 Hz without specifying the isoform ([4] and private communication). Adamo *et al.* made direct measurements of the turnover rate and determined it to be 33 Hz for the erythrocyte PMCA [29]. However, the calculated turnover rates, even being in the appropriate range, may differ from the presented values since the expression levels of the pump can not be determined with much accuracy, and factors such as other proteins and lipids interacting with the pump in the biological membrane environment can have substantial effects.

For comparison, the turnover rate of the Sarcoplasmic Reticulum Ca^{2+}-ATPase (SERCA) lies within the same range. The SERCA1, SERCA2a and SERCA3 isoforms transport calcium with a turnover rate of $\approx$ 10 Hz, whereas the the SERCA2b isoform exhibits a rate of $\approx$ 5 Hz [22]. Note that in contrast to the PMCA the SERCA carries two calcium ions per pump cycle reflected in the Ca^{2+}:ATP stoichiometry of 2:1 [7, 22].

The isoform specific universal set of parameters may be applied to different scenarios by incorporating the system specific expression levels of PMCA. However, alterations of the stimulation rate constants may occur under modified experimental conditions. Since we consider proteins with polar binding sites we cannot exclude a change of dynamical properties at different ionic strengths of the experimental solutions. Corresponding experiments could elucidate the importance of such effects. Also our theoretical proposition of the

calmodulin dependence of the stimulation and the relaxation constant which differs from the linear behavior found by Caride *et al.* calls for further experimental investigations.

Acknowledgment

This work has been completed during support of Michael Graupner by a French Government scholarship in conjunction with a DAAD supplement and during support of M. Meyer-Hermann by a Marie Curie Intra-European Fellowship within the Sixth EU Framework Programme. We are indebted to Ariel Caride for kindly providing us the data and fruitful communications. We also would like to thank Jakob Schweizer and Nicolas Brunel for many discussions. Furthermore we want to thank Alexander Roxin for revising the manuscript.

Appendix

Stimulation model By using the Law of Mass Action the stimulation model (1)-(5) is rewritten as a set of differential equations for concentrations

$$\frac{dP}{dt} = -\frac{k_2 P(M_0 - P_X - P_X^*)}{1 + 1/(KCa^4)} + k_{-2} P_X + k_5(P_0 - P - P_X - P_X^*), \tag{16}$$

$$\frac{dP_X}{dt} = \frac{k_2 P(M_0 - P_X - P_X^*)}{1 + 1/(KCa^4)} - (k_{-2} + k_3) P_X, \tag{17}$$

$$\frac{dP_X^*}{dt} = k_3 P_X - k_4 P_X^* + k_{-4}(P_0 - P - P_X - P_X^*) \frac{M_0 - P_X - P_X^*}{1 + 1/(KCa^4)}. \tag{18}$$

Pump conservation $P_0 = P + P_X + P_X^* + P^*$ where P_0 is the total pump concentration and calmodulin conservation $M_0 = M + X_4 + P_X + P_X^*$ with M_0 as total calmodulin concentration is respected. We solve this system of coupled ordinary differential equations of first order with a fourth-order Runge-Kutta method. This has been implemented in a C++ program.

Hill fit of the stimulation constant The data from [9] can be fitted by the Hill equation

$$k_{\text{stim}}^{\text{exp}}(Ca) = \frac{k_{\text{stim}}^{\max} \cdot Ca^4}{{Ca_{\text{stim}}^{(1/2)}}^4 + Ca^4}, \tag{19}$$

with the maximal stimulation constant $k_{\text{stim}}^{\max}$ and the half maximum concentration $Ca_{\text{stim}}^{(1/2)}$. According to (6), $k_{\text{stim}}^{(3)}$ converges to k_3 for large calcium or calmodulin concentrations (see below), hence k_3 confines the maximum stimulation rate and can be identified with $k_{\text{stim}}^{\max}$.

This reflects the fact that equation (3) limits the stimulation rate. By setting the right hand side of equation (6) equal to $k_3/2$, an expression for the Ca^{2+} concentration at half maximal stimulation is derived

$$Ca_{\text{stim}}^{(1/2)} = \sqrt[4]{\frac{k_{-2} + k_3/2}{k_2 \cdot K \cdot M}}. \tag{20}$$

Note that the calmodulin concentration M is kept constant.

In a similar manner, the experimental relaxation constants can be fitted by an inverse Hill equation. Note that we expect the dependence of the stimulation and relaxation constant on calmodulin to be fitted by a Hill equation with Hill coefficient 1.

Limes of equation (6) We consider the limes of $k_{\text{stim}}^{(2/3)}$ for $X_4 \to \infty$ in the case of real and positive rate constants k_2, k_{-2} and k_3.

$$\begin{aligned} \lim_{X_4\to\infty} k_{\text{stim}}^{(2/3)} &= \lim_{X_4\to\infty} \frac{k_{-2} + k_3 + k_2X_4}{2} \pm \sqrt{\left(\frac{k_{-2} + k_3 + k_2X_4}{2}\right)^2 - k_2k_3X_4} \\ &= \lim_{X_4\to\infty} \frac{k_{-2} + k_3 + k_2X_4}{2} \left(1 \pm \sqrt{1 - \frac{4k_2k_3X_4}{(k_{-2} + k_3 + k_2X_4)^2}}\right) \end{aligned} \tag{21}$$

For $k_{\text{stim}}^{(2)}$ this expression diverges, whereas we find $\lim_{X_4\to\infty} k_{\text{stim}}^{(3)} = k_3$ using the rule of de l'Hospital.

References

[1] L. Zylinska and M. Soszynski, *Plasma membrane Ca^{2+}-ATPase in excitable and nonexcitable cells*, Acta Biochim. Pol. **47**, 529 (2000).

[2] J. T. Penniston and A. Enyedi, *Modulation of the plasma membrane Ca^{2+} pump*, J. Membr. Biol. **165**, 101 (1998).

[3] E. Carafoli, *The calcium pumping ATPase of the plasma membrane*, Annu. Rev. Physiol. **53**, 531 (1991).

[4] M. Juhaszova, P. Church, M. P. Blaustein, and E. F. Stanley, *Location of calcium transporters at presynaptic terminals*, Eur. J. Neurosci. **12**, 839 (2000).

[5] D. Guerini, *The significance of the isoforms of plasma membrane calcium ATPase*, Cell Tissue Res. **292**, 191 (1998).

[6] T. P. Stauffer, D. Guerini, and E. Carafoli, *Tissue distribution of the four gene products of the plasma membrane calcium pump*, J. Biol. Chem. **270**, 12184 (1995).

[7] E. Carafoli, *The Ca^{2+} pump of the plasma membrane*, J. Biol. Chem. **267**, 2115 (1992).

[8] D. Chin and A. R. Means, *Calmodulin: a prototypical calcium sensor*, Trends Cell Biol. **10**, 322 (2000).

[9] A. J. Caride, A. R. Penheiter, A. G. Filoteo, Z. Bajzer, A. Enyedi, and J. T. Penniston, *The plasma membrane calcium pump displays memory of past calcium spikes*, J. Biol. Chem. **276**, 39797 (2001).

[10] S. Linse, A. Helmersson, and S. Forsen, *Calcium binding to calmodulin and its globular domains*, J. Biol. Chem. **266**, 8050 (1991).

[11] W. J. Pottorf, S. P. Duckles, and J. N. Buchholz, *Mechanisms of calcium buffering in adrenergic neurones and effects of ageing: testing the limits of homeostasis*, J. Auton. Pharmacol. **20**, 63 (2000).

[12] A. Persechini and B. Cronk, *The relationship between the free concentrations of Ca^{2+} an Ca^{2+}-calmodulin in intact cells*, J. Biol. Chem. **274**, 6827 (1999).

[13] T. Meyer, P. I. Hanson, L. Stryer, and H. Schulman, *Calmodulin trapping by calcium-calmodulin-dependent protein kinase*, Science **256**, 1199 (1992).

[14] A. Persechini, K. Yano, and P. M. Stemmer, *Ca^{2+} binding and energy coupling in the calmodulin-myosin light chain kinase complex*, J. Biol. Chem. **275**, 4199 (2000).

[15] N. L. Elwess, A. G. Filoteo, A. Enyedi, and J. T. Penniston, *Plasma membrane Ca^{2+} pump isoforms 2a and 2b are unusually responsive to calmodulin and Ca^{2+}*, J. Biol. Chem. **272**, 17981 (1997).

[16] A. R. Penheiter, B. Zeljko, A. G. Filoteo, R. Thorogate, K. Török, and A. J. Caride, *A model of the activation of plasma membrane calcium pump isoform 4b by calmodulin*, J. Bio. Chem. **42**, 12115 (2003).

[17] A. J. Caride, A. G. Filoteo, N. L. Elwess, A. K. Verma, A. Enyedi, Z. Bajzer, and J. T. Penniston, *The rate of activation by calmodulin of isoform 4 of the plasma membrane*

Ca^{2+} pump is slow ans is changed by alternative splicing, J. Biol. Chem. **274**, 35227 (1999).

[18] A. Enyedi, A. G. Filoteo, G. Gardos, and J. T. Penniston, *Calmodulin-binding domains from isozymes of the plasma membrane calcium pump have different regulatory properties*, J. Biol. Chem. **266**, 8952 (1991).

[19] W. Ba-Thein, A. J. Caride, A. G. Filoteo, A. Enyedi, K. Paszty, C. L. Croy, and J. T. Penniston, *Chimaeras reveal the role of the catalytic core in the activation of the plasma membrane Ca^{2+} pump*, Biochem. J. **356**, 241 (2001).

[20] A. R. Penheiter, A. J. Caride, A. Enyedi, and J. T. Penniston, *Tryptophan 1093 is largely responsible for the slow off rate off calmodulin from plasma membrane calcium pump 4b*, J. Biol. Chem. **277**, 17728 (2002).

[21] A. J. Caride, A. G. Filoteo, A. R. Penheiter, K. Paszty, A. Enyedi, and J. T. Penniston, *Delayed activation of the plasma membrane calcium pump by a sudden increase in Ca^{2+}: fast pumps reside in fast cells*, Cell Calcium **30**, 49 (2001).

[22] J. Lytton, M. Westlin, S. E. Burk, G. E. Shull, and D. H. MacLennan, *Functional comparisions between isoforms of the sacroplasmic or endoplasmic reticulum family of calicum pumps*, J. Biol. Chem. **267**, 14483 (1992).

[23] A. K. Verma, A. Enyedi, A. G. Filoteo, E. E. Strehler, and J. T. Penniston, *Plasma membrane calcium pump isoform 4a has a longer calmodulin-binding domain than 4b*, J. Biol. Chem. **271**, 3713 (1996).

[24] H. Hilfiker, D. Guerini, and E. Carafoli, *Cloning and expression of the isoform 2 ot the human plasma membrane Ca^{2+} ATPase*, J. Biol. Chem. **269**, 26178 (1994).

[25] H. P. Adamo and M. E. Grimaldi, *Functional consequences of relocation the c-terminal calmodulin-binding autoinhibitory domains of the plasma membrane Ca^{2+} pump near the n-terminus*, Biochem. J. **331**, 763 (1998).

[26] A. Hudmon and H. Schulman, *Neuronal Ca^{2+}/calmodulin-dependent protein kinase II: The role of structure and autoregulation in cellular function*, Annu. Rev. Biochem. **71**, 473 (2002).

[27] B. B. Olwin, A. M. Edelman, E. G. Krebs, and D. R. Strom, *Quantitation of energy coupling between Ca2+, calmodulin, skeletal muscle myosin light chain kinase, and kinase substrates*, J. Biol. Chem. **259**, 10949 (1984).

[28] D. Guerini, A. Zecca-Mazza, and E. Carafoli, *Single amino acid mutations in transmembrane domain 5 confer to the plasme membrane Ca^{2+} pump properties typical of the Ca^{2+} pump of endo(sacro)plasmic reticulum*, J. Bio. Chem. **275**, 31361 (2000).

[29] H. Adamo, A. Rega, and P. Garrahan, *Pre-steady-state phosphorylation of the human red cell Ca2+-ATPase*, J. Bio. Chem. **263**, 17548 (1988).

Tables

parameter	**h2b**	**h4b**	**unit**	**source**
K	> 0.029		$1/\mu\mathrm{M}^4$	see text
k_3	0.055	0.024	1/s	$k_{\mathrm{stim}}^{\mathrm{max}}$
k_4	0.015	0.0347	1/s	$k_{\mathrm{relax}}^{\mathrm{exp}}$

Table 1: **Stimulation parameters and ranges determined by Hill equation fits** Pump specific rate constants and ranges determined by fits of the Hill equation to the experimental data from Caride *et al.* (2001) [9].

parameter	**h2b**	**c.i.(68%)**	**h4b**	**c.i.(68%)**	**unit**
k_2	1.99	1.92...8.91	0.096	0.088...0.168	$1/(\mu\mathrm{M}\cdot\mathrm{s})$
k_3	0.056	0.053...0.058	0.023	0.021...0.025	1/s
k_4	0.016	0.015...0.052	0.035	0.035...0.147	1/s
k_{-4}	20001	19988...20010	19999	19978...20017	$1/(\mu\mathrm{M}\cdot\mathrm{s})$
k_5	0.12	0.02...0.35	0.84	0.14...0.97	1/s

Table 2: **Determination of stimulation parameters with a Metropolis algorithm** The medians and the confidence intervals (c.i.) of 68 % are calculated with a Bootstrap method combined with a Metropolis algorithm using experimental data for the stimulation constant, relaxation constant and steady-state pumping activity (see text for more details). K is chosen to be 1 $\mu\mathrm{M}^{-4}$. k_{-2} can be calculated from k_2 using the known dissociation constant $K_2 = k_{-2}/k_2$ (see text).

parameter	**h2b**			**h4b**			**unit**
K	0.1	1	10	0.1	1	10	$1/\mu\mathrm{M}^4$
k_2	24.8	1.99	0.20	1.46	0.096	0.0093	$1/(\mu\mathrm{M}\cdot\mathrm{s})$
k_3	0.058	0.056	0.056	0.023	0.023	0.023	$1/\mathrm{s}$
k_4	0.015	0.016	0.018	0.036	0.035	0.035	$1/\mathrm{s}$
k_{-4}	19991	20001	20001	19993	19999	19998	$1/(\mu\mathrm{M}\cdot\mathrm{s})$
k_5	0.019	0.12	0.68	0.06	0.84	7.4	$1/\mathrm{s}$
J^*_{max}	0.24	0.24	0.24	0.73	0.73	0.76	$\frac{\mu\mathrm{mol}}{\mathrm{mg}\cdot\mathrm{min}}$
$H^*_{1/2}$	0.44	0.45	0.45	0.56	0.57	0.54	$\mu\mathrm{M}$

Table 3: **Parameters at different values of K**

See table 2, 4 and the text for more details concerning the determination of these values.

parameter	**h2b**	**c.i.**(%**68**)	**h4b**	**c.i.**(%**68**)	**unit**	**characteristic**
J_{max}	$0.116\,(48\%\,of\,J^*_{\mathrm{max}})$	± 0.008	$0.148\,(20\%\,of\,J^*_{\mathrm{max}})$	± 0.018	$\frac{\mu\mathrm{mol}}{\mathrm{mg}\cdot\mathrm{min}}$	system specific
J_{single}	5.0	± 0.3	6.4	± 0.8	Hz	universal
J^*_{max}	0.24	0.23...0.26	0.73	0.68...0.75	$\frac{\mu\mathrm{mol}}{\mathrm{mg}\cdot\mathrm{min}}$	system specific
J^*_{single}	10.4	10.0...11.3	31.7	29.5...32.5	Hz	universal
$H_{1/2}$	0.63	± 0.07	1.45	± 0.26	$\mu\mathrm{M}$	universal
$H^*_{1/2}$	0.45	0.29...0.53	0.57	0.46...0.62	$\mu\mathrm{M}$	universal

Table 4: **Pumping parameters**

Parameters of the steady-state pump activity determined using experimental data of Caride *et al.* 2001 [9]. K is chosen to be 1 $\mu\mathrm{M}^{-4}$. The activity values in the absence of calmodulin are determined by a gnuplot fit to the experimental data. The medians and the confidence intervals (c.i.) of J^*_{max} and $H^*_{1/2}$ are derived from a Bootstrap method combined with the Metropolis algorithm (see text for more details).

Figure legends

Figure 1 $k^{(3)}_{\mathrm{stim}}$ is plotted against calcium at constant calmodulin concentration of 0.117 μM for isoforms h2b and h4b according to equation (6) (full lines). The dotted lines represent the $k^{(3)}_{\mathrm{stim}}$ dependence on calmodulin at fixed calcium concentration of 0.8 μM for the h2b and 1 μM for the h4b isoform. The stimulation rate $k^{\mathrm{exp}}_{\mathrm{stim}}$ (squares) has been measured at various calcium concentration with constant calmodulin concentration of 0.117 μM (with kind permission of Caride [9]).

Figure 2 The relaxation constant k_{relax} is plotted for varying calcium (full lines) and calmodulin (dotted lines) concentrations where calmodulin ($M = 0.117$ μM for both isoforms) and calcium ($Ca = 0.25$ μM for h2b; $Ca = 0.3$ μM for h4b) are kept constant, respectively. Corresponding measurements at $M = 0.117$ μM are shown (squares). With kind permission of Caride [9].

Figure 3 The dynamics of the fractions $f_{\mathrm{unstim}} = \frac{P+P_X}{P_0}$ (full lines for h2b, dashed-dotted lines for h4b) and $f_{\mathrm{stim}} = \frac{P^*+P^*_X}{P_0}$ (dashed lines for h2b, dotted lines for h4b) are shown during stimulation (panel (a)) and relaxation (panel (b)). The total calmodulin concentration is 0.117 μM and $P_0 = 0.005\,\mu$M. Note that the formation and degradation of stimulated and unstimulated pump form depend on the available calcium and calmodulin concentration. The present calcium concentration is 0.5 μM during stimulation (a) and 0.1 μM during relaxation (b).

Figure 4 Steady-state calcium dependent pump activity of both isoforms. The measurements in the absence (triangles) and in the presence (circles) of $0.117\,\mu$M calmodulin have been kindly provided by Caride [9]. The total pump concentration P_0 is taken from [9] to be $0.005\,\mu$M. Without calmodulin (full line) the fit of equation (13) to the data displays no difference to the fit of the simplified equation (14) which presumes a cooperative binding. Therefore, only the fit of equation (14) is shown. The dashed line shows the realistic case and displays $f_{\mathrm{stim}} \simeq 0$ for low calcium concentrations. The dashed-dotted line depicts the pump activity with the assumption that only stimulated pump form is present at all calcium concentrations, *i.e.* $f_{\mathrm{stim}} = 1$ and $f_{\mathrm{unstim}} = 0$.

Figure 5 The fractional calmodulin dependent steady-state pump activity $f = (J - J_{\max})/(J^*_{\max} - J_{\max})$ of the h4b isoform at $Ca = 0.7$ μM is shown. $J_{\max}$ is the activity in the absence of calmodulin and $J^*_{\max}$ is the steady-state activity in the presence of saturating calmodulin, both at the accordant calcium concentration of 0.7 μM. The calculation has been done with $P_0 = 0.005$ μM.

Figure 6 Figure (a) shows the theoretical (full line) and the experimentally measured (crosses) time course of Ph_i production during different calcium concentration exposures, shown on the top of the panel. The present calmodulin concentration was 0.117 μM. Figure (b) shows the fraction of change in $J_{0.05}$, $\left(\frac{J^{(\mathrm{second})}_{0.05} - J^{(\mathrm{first})}_{0.05}}{\Delta J}\right)$ as a function of time at low calcium (0.05 μM), experimentally measured (crosses) and theoretically predicted (full line). Both experiments were performed with the h2b isoform (with kind permission of Caride [9]).

Figures

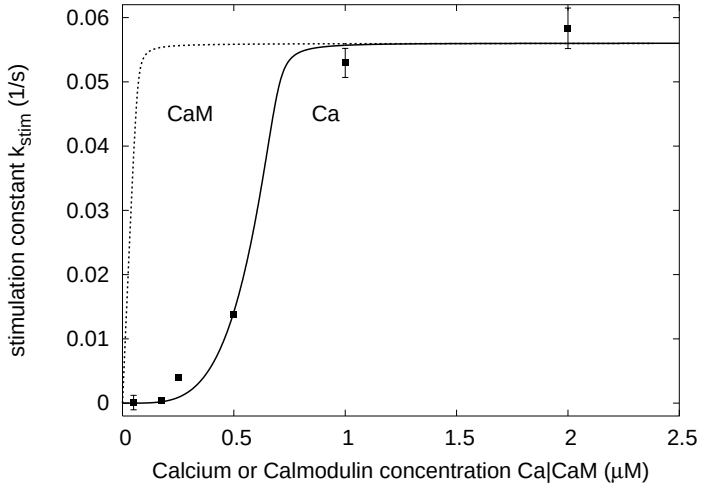

(a) h2b isoform

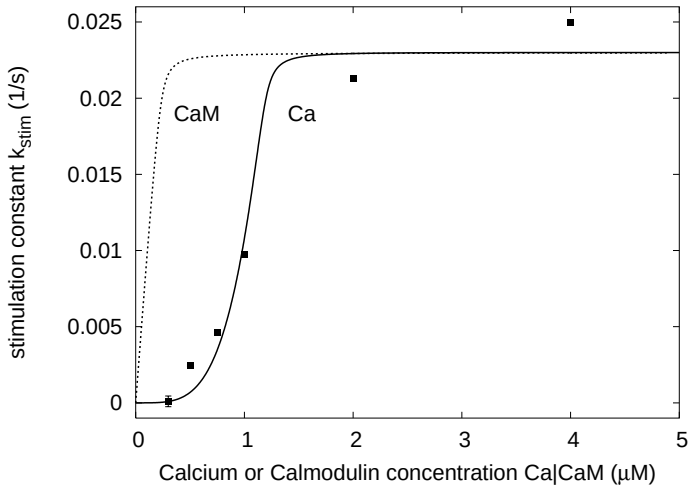

(b) h4b isoform

Figure 1:

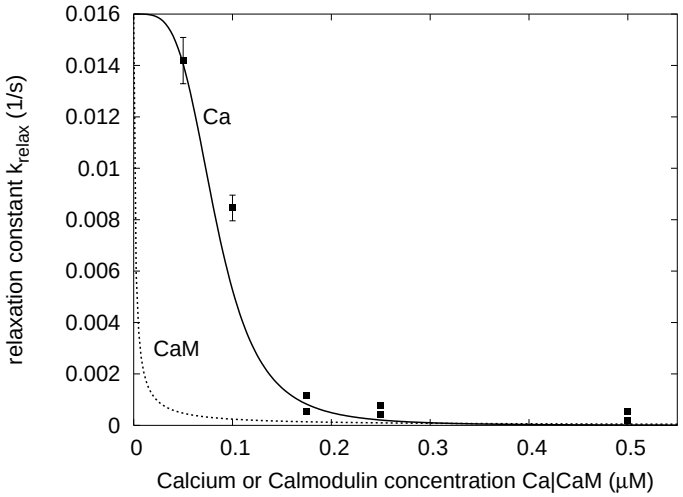

(a) h2b isoform

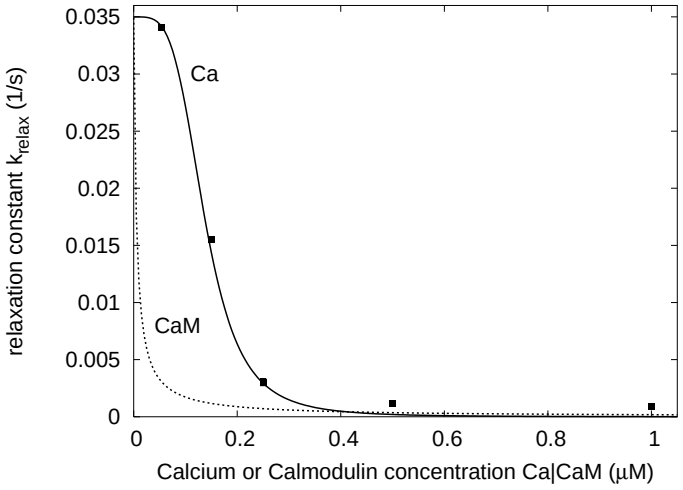

(b) h4b isoform

Figure 2:

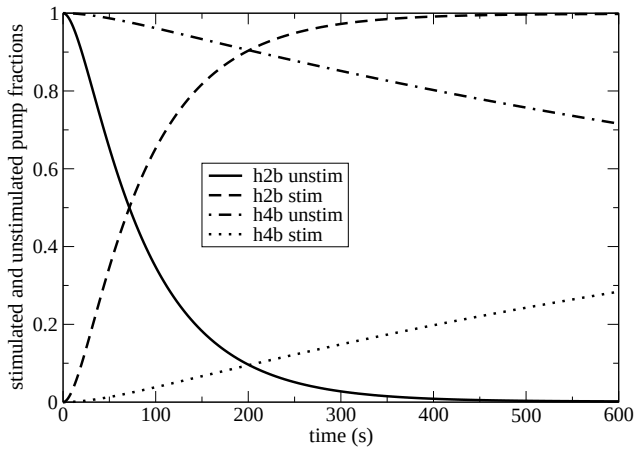

(a) stimulation

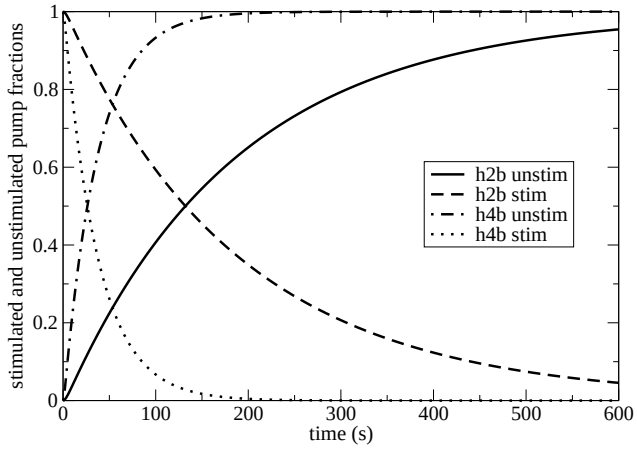

(b) relaxation

Figure 3:

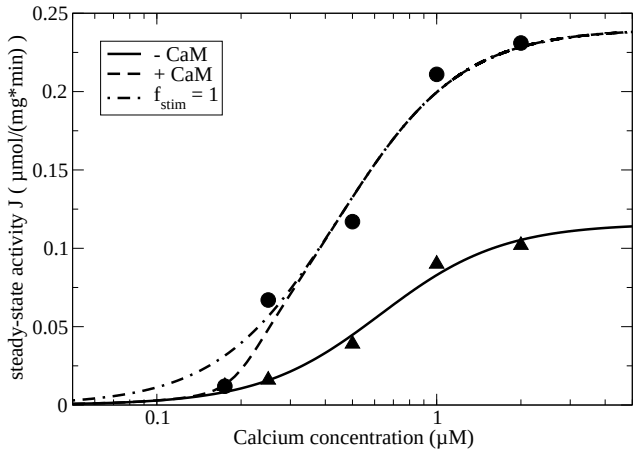

(a) h2b isoform

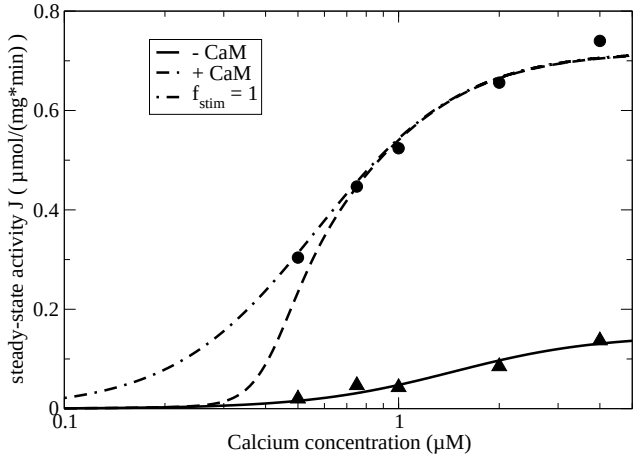

(b) h4b isoform

Figure 4:

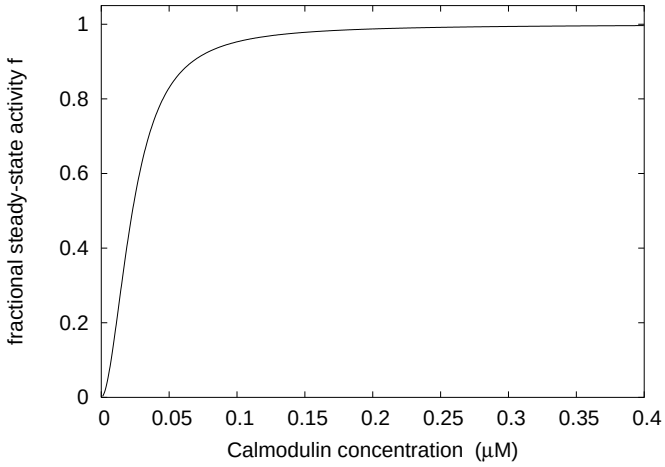
fractional steady-state activity f
1
0.8
0.6
0.4
0.2
0
0
0.05
0.1
0.15
0.2
0.25
0.3
0.35
0.4
Calmodulin concentration (μM)

Figure 5:

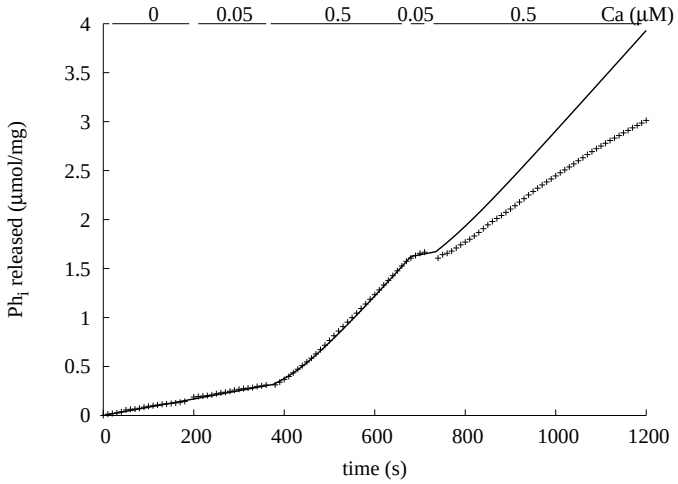

(a) time course of Ph_i production

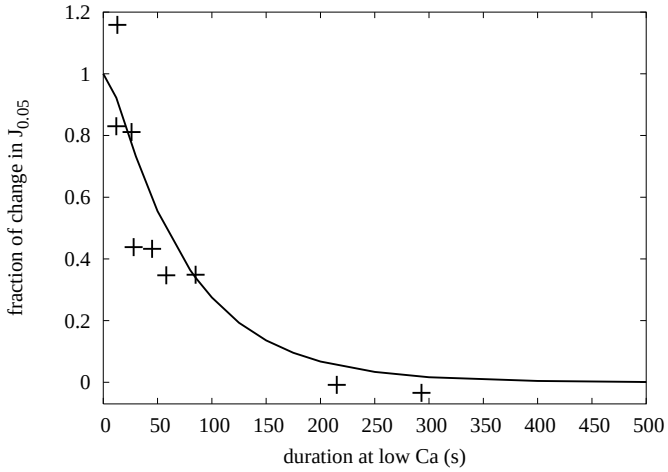

(b) fraction of change in $J_{0.05}$

Figure 6: